

Low-temperature (4.2°K) study of the ${}^2E_{1u} \leftarrow {}^2E_{2g}$ band system in the electronic spectra of various ferricenium compounds

David N. Hendrickson*, Y. S. Sohn†, D. Michael Duggan*‡, and Harry B. Gray†

William A. Noyes Laboratory, University of Illinois, Urbana, Illinois 61801

The Arthur Amos Noyes Laboratory of Chemical Physics, California Institute of Technology, Pasadena, California 91109 §

(Received 10 August 1972)

The ${}^2E_{1u} \leftarrow {}^2E_{2g}$ (16 200 cm^{-1}) band system for the three ferricenium salts $[\text{Fe}(\text{C}_5\text{H}_5)_2]\text{PF}_6$, $[\text{Fe}(\text{C}_5\text{H}_5)_2]\text{BF}_4$, and $[\text{Fe}(\text{C}_5\text{H}_5)_2](\text{CCl}_3\text{CO}_2\text{H})_2-(\text{CCl}_3\text{CO}_2^-)$ has been studied at 4.2°K. Analysis of the observed vibrational structure indicates that the ${}^2E_{1u}$ excited state is split into two Kramers doublets, with the extent of splitting being a function of the anion. Several ferricenium ${}^2E_{1u}$ vibrational frequencies have been identified and compared with corresponding values for ground state ferrocene. It appears from these comparisons that the iron $4p_x$ and $4p_y$ orbitals are minimally involved in the iron-ring bonding.

INTRODUCTION

Variable-temperature magnetic susceptibility¹ and ESR²⁻⁴ studies have shown that the ferricenium ion has a ${}^2E_{2g}(a_{1g})^2(e_{2g})^3$ ground state, which is split into two Kramers doublets by spin-orbit coupling and crystal fields of symmetry lower than D_5 . The magnitude of the low-symmetry crystal field splitting was found to be comparable to the spin-orbit interaction in the cation, and further, it was found to be a function of ring substitution and ferricenium environment (anion or solvent).

Studies of the electronic absorption spectrum of the ferricenium ion have emphasized⁵⁻⁷ the characterization of band system *I*, which peaks at approximately 16 200 cm^{-1} . The accumulated experimental evidence has now firmly established,⁵⁻⁷ contrary to earlier suggestions,^{8,9} that the band arises from the ligand-to-metal charge transfer transition ${}^2E_{1u} \leftarrow {}^2E_{2g}$. The vibrational structure resolved in the 16 200 cm^{-1} band system for various ferricenium salts in KBr pellets at 77°K indicates that the ${}^2E_{1u}$ excited state is split into two Kramers doublets by low-symmetry crystal field components.⁷ We have now extended the electronic absorption spectral investigation of band system *I* to lower temperatures for three ferricenium salts, $[\text{Fe}(\text{C}_5\text{H}_5)_2]\text{PF}_6$, $[\text{Fe}(\text{C}_5\text{H}_5)_2](\text{CCl}_3\text{CO}_2\text{H})_2(\text{CCl}_3\text{CO}_2^-)$, and $[\text{Fe}(\text{C}_5\text{H}_5)_2]\text{BF}_4$. The very significantly improved resolution of the band system obtained at 4.2°K has allowed a more detailed characterization of the ${}^2E_{1u}$ excited state of the ferricenium ion.

EXPERIMENTAL

Ferrocene was purified by recrystallization from ethanol followed by sublimation in vacuum. Samples of $[\text{Fe}(\text{C}_5\text{H}_5)_2]\text{PF}_6$ and $[\text{Fe}(\text{C}_5\text{H}_5)_2]\text{BF}_4$ were prepared as described previously.^{1,7} Large single crystals of $[\text{Fe}(\text{C}_5\text{H}_5)_2](\text{CCl}_3\text{CO}_2\text{H})_2(\text{CCl}_3\text{CO}_2^-)$ were grown by slow evaporation of a benzene solution of ferrocene and trichloroacetic acid and these were used in the

optical studies. It has been suggested¹⁰ that the ferricenium and cobalticenium trichloroacetic acid salts contain the radical anion $(\text{CCl}_3\text{CO}_2\text{H})_2^-$. In a recent article,¹¹ the existence of a radical anion was questioned. We have carried out careful potentiometric titrations of various samples of the ferricenium trichloroacetate salt that we prepared. Three methods were used to prepare the samples:

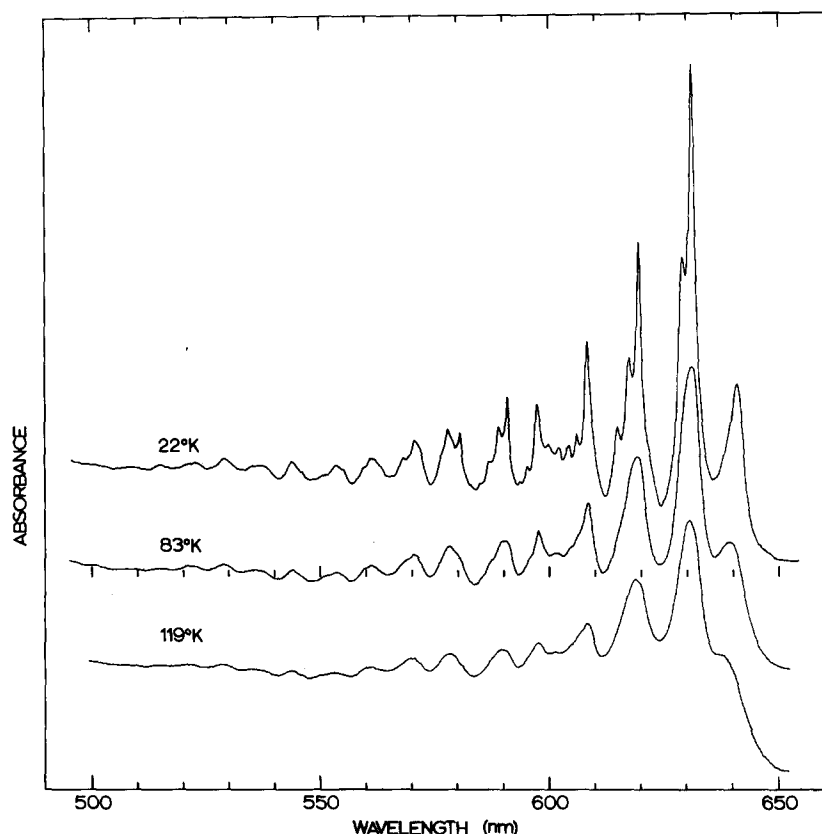
(1) Slow evaporation of a benzene solution, as described above.

(2) Oxidation of ferrocene with conc H_2SO_4 , followed by dilution with water, and then precipitation with trichloroacetic acid.

(3) Dissolution of ferrocene and trichloroacetic acid in benzene, followed by bubbling with oxygen, and then stoppering the flask until small crystals formed. Titration with 0.01*N* NaOH produced sharp curves with a $\text{H}^+/\text{ferricenium}$ ratio of 2.11 ± 0.05 . It is known that the ferricenium ion is unstable in basic media and that in water OH^- is consumed in the ferricenium decomposition. Thus, slight decomposition during the titration could account for the fact that our $\text{H}^+/\text{ferricenium}$ ratios were all slightly greater than 2.00. In fact, we found that if the titration was carried out over longer periods (> 2 h) the $\text{H}^+/\text{ferricenium}$ ratio approached 3.0. In summary, we believe that the ferricenium samples used in our investigation were trichloroacetate salts.

The electronic absorption spectra of $[\text{Fe}(\text{C}_5\text{H}_5)_2]\text{PF}_6$ were recorded for 13 mm KBr pellets on a Cary Model 14 CMRI spectrophotometer. The variable-temperature runs were completed using a Spectrim cryocooling module (Cryogenic Technology, Incorporated). This unit adapted easily to the Cary and provided rapid cool down of low-mass sample configurations to a minimum of 16°K. The KBr pellets of the PF_6^- salt were also immersed directly in liquid helium contained in a glass Dewar and run on the Cary. The BF_4^- ferricenium salt was not very stable pelleted in KBr and in this case spectra were taken on the Cary of a

FIG. 1. Vibrational structure of band system I for a KBr pellet of $[\text{Fe}(\text{C}_6\text{H}_5)_2]\text{PF}_6$ at three temperatures (Cary 14 data).



Nujol mineral oil mull, which was sandwiched between quartz plates immersed in liquid helium.

In an effort to obtain improved resolution, spectra of KBr pellets of the PF_6^- salt and single crystals of the trichloroacetate salt were recorded photographically (Kodak 103a-F plates) in second order on a Jarrell-Ash 0.75-m instrument equipped with a grating blazed at $10\,000\text{ \AA}$. The exposed plates were traced on a Jarrell-Ash densitometer. Several KBr pellets (different concentrations) as well as KCl and NaCl pellets of the PF_6^- salt were run. In all cases, the samples were directly immersed in liquid helium. A mercury arc was used for calibration purposes.

RESULTS AND DISCUSSION

$[\text{Fe}(\text{C}_6\text{H}_5)_2]\text{PF}_6$

The temperature dependence (119–22°K) of band system I in the spectrum of a KBr pellet of $[\text{Fe}(\text{C}_6\text{H}_5)_2]\text{PF}_6$ is depicted in Fig. 1. Liquid helium electronic absorption spectra were measured for KBr pellets of this compound both on Cary 14 and 0.75-m Jarrell-Ash instruments. These spectra are reproduced in Figs. 2–4. Two different pellet concentrations were used to obtain the spectra shown in Figs. 3 and 4 to keep most of the desired density information within the workable range of the films. Table I lists the peak positions measured from Figs. 3 and 4.

We must first comment on the seeming discrepancy between certain regions of Figs. 2 and 3, in particular the splittings of the second and third band groups, and the intensity of the 6412-\AA peak. In the Cary 14 spectrum (Fig. 2), the band group at $\sim 630\text{ nm}$ appears as two peaks while the band group at $\sim 630\text{ nm}$ in the Jarrell-Ash spectrum consists of three peaks and at least one shoulder. It is clear that better resolution was obtained on the Jarrell-Ash instrument than on the Cary 14. Even further, we have found that it is possible using a Dupont curve synthesizer to increase artificially the peak widths in the 630-nm Jarrell-Ash band group (Fig. 3) to give a spectrum similar in the 630-nm region to that obtained on the Cary 14 (Fig. 2).

The difference in relative intensities of the lowest energy peaks (compare Figs. 2 and 3) is hard to explain with certainty. One possible explanation is that the resolution of the 0.75-m instrument is sufficient to separate the 6412-\AA peak from the second grouping, decreasing the overlap of the two band groups, and resulting thus in an apparent loss in relative intensity of the 6412-\AA peak. There is perhaps a more probable explanation entailing a consideration of film exposure. In order to record the more intense absorptions photographically (Fig. 3), the low energy end of the spectrum was overexposed and "blocking" of the silver grains causes a large part of the absorption contour of the 6412-\AA band to be lost in an artificially raised base line.

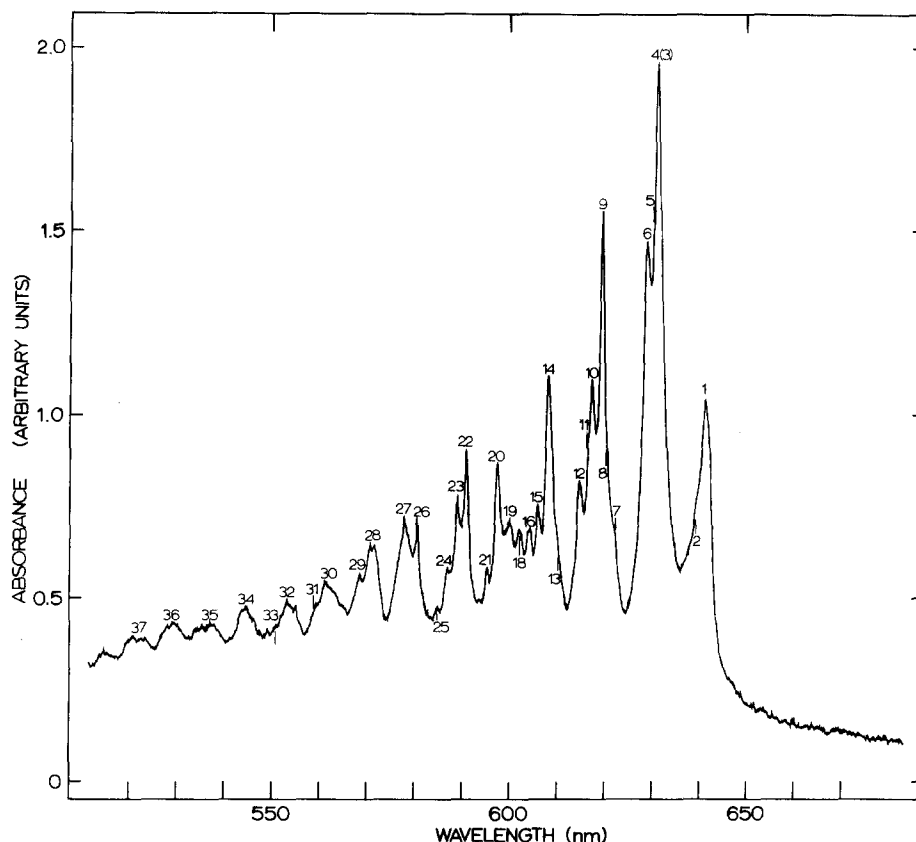


FIG. 2. Band system *I* for a medium concentration KBr pellet of $[\text{Fe}(\text{C}_5\text{H}_5)_2]\text{PF}_6$ at 4.2°K (Cary 14 data).

In summary, we believe that Fig. 3 exhibits the best resolution, whereas Fig. 2 gives the best relative intensity data for band system *I* in the 4.2°K spectrum of $[\text{Fe}(\text{C}_5\text{H}_5)_2]\text{PF}_6$.

In assigning the vibrational structure of the band *I* system of the ferricenium ion, reference will be made to the observed gerade vibrational modes of ground state ferrocene.¹²⁻¹⁴ The positions and descriptions of these modes are set out in Table II. The low-concentration, 4.2°K spectrum of $[\text{Fe}(\text{C}_5\text{H}_5)_2]\text{PF}_6$ exhibits what appears to be a 300-cm^{-1} progression of a multiplet of four

or more peaks (Fig. 3). Individual $\sim 300\text{-cm}^{-1}$ vibrational progressions can be seen in the spectrum. The 300-cm^{-1} frequency is assigned to the totally symmetric a_{1g} ring-metal-ring stretch ν_4 ; four progressions of this frequency are noted in Table I. The lowest-energy 300-cm^{-1} progression seems to originate with the low-intensity $15\,596\text{-cm}^{-1}$ peak, and this origin is designated as *A*(1). The electronic origin *A*(1) corresponds to the transition from the lowest-energy ground state Kramers doublet to the lowest-energy ${}^2E_{1u}$ excited state Kramers doublet. Assignment of the peak position for the transi-

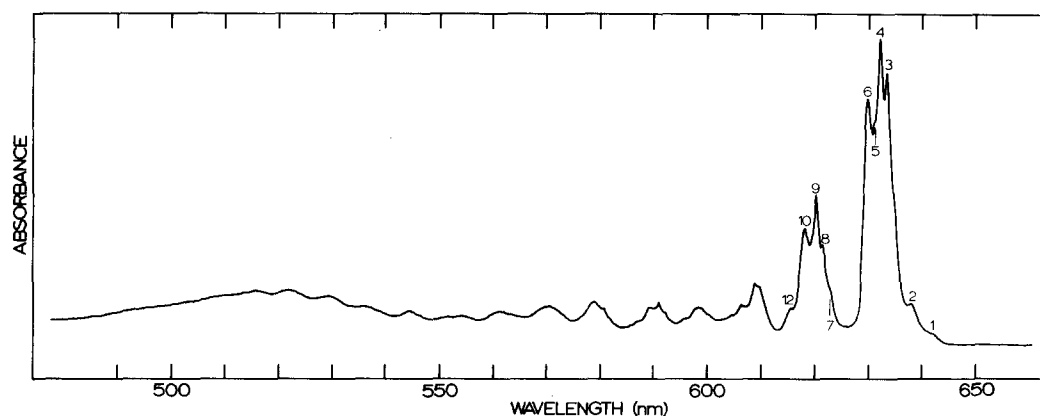


FIG. 3. Band system *I* for a low concentration KBr pellet of $[\text{Fe}(\text{C}_5\text{H}_5)_2]\text{PF}_6$ at 4.2°K (Jarrell-Ash data).

TABLE I. Vibrational structure of band system I observed for $[\text{Fe}(\text{C}_5\text{H}_5)_2]\text{PF}_6$ as a KBr pellet at 4.2°K.

Band label	λ (Å)	$\bar{\nu}$ (cm^{-1}) $\pm 5 \text{ cm}^{-1}$	$\Delta\bar{\nu}(a)$ $\pm 10 \text{ cm}^{-1}$	$\Delta\bar{\nu}(b)$ $\pm 10 \text{ cm}^{-1}$	$\Delta\bar{\nu}(c)$ $\pm 10 \text{ cm}^{-1}$	$\Delta\bar{\nu}(d)$ $\pm 10 \text{ cm}^{-1}$	Assignments
1	6412	15 596	origin				$A(1)$
2	6374(sh)	15 689					
3	6330	15 798					
4	6316	15 833		origin			$A(2)$
5	6308(sh)	15 853					
6	6295	15 886	290				$A(1) + \nu_4$
7	6223(sh)	16 069					
8	6214	16 093					
9	6200	16 129		296			$A(2) + \nu_4$
10	6180	16 181	295				$A(1) + 2\nu_4$
11	6167(sh)	16 215					
12	6153	16 252					
13	6098(sh)	16 399					
14	6085	16 434		305			$A(2) + 2\nu_4$
15	6062	16 496	315				$A(1) + 3\nu_4$
16	6045	16 542					
17	6040(sh)?	16 556					
18	6023	16 603			origin		$A(2) + \nu_x$
19	6001	16 664					$A(1) + \nu_x + \nu_4$
20	5976	16 734		300			$A(2) + 3\nu_4$
21	5955	16 793	297				$A(1) + 4\nu_4$
22	5910	16 920			317		$A(2) + \nu_x + \nu_4$
23	5891	16 975				311	$A(1) + \nu_x + 2\nu_4$
24	5869	17 039		305			$A(2) + 4\nu_4$
25	5850	17 094	301				$A(1) + 5\nu_4$
26	5808	17 226			306		$A(2) + \nu_x + 2\nu_4$
27	5781	17 298				323	$A(1) + \nu_x + 3\nu_4$
28	5709	17 516			290		$A(2) + \nu_x + 3\nu_4$
29	5685	17 590				292	$A(1) + \nu_x + 4\nu_4$
30	5615	17 809			293		$A(2) + \nu_x + 4\nu_4$
31	5600(sh)	17 857				267	$A(1) + \nu_x + 5\nu_4$
32	5541	18 047					
33	5515(sh)	18 132			323		$A(2) + \nu_x + 5\nu_4$
34	5445	18 365					
35	5373	18 612					
36	5299	18 871					
37	5227	19 131					

tion to the other ${}^2E_{1u}$ doublet is difficult. In Table I, we have tentatively assigned, on the basis of intensities, the $A(2)$ origin to the 15 833- cm^{-1} peak. This assignment gives a $\sim 240\text{-cm}^{-1}$ splitting in the ${}^2E_{1u}$ excited state due to low-symmetry crystal fields. A 300- cm^{-1} progression develops from the assigned $A(2)$ origin. The over-all band shape and the observation of both the $A(1)$ and $A(2)$ $\sim 300\text{-cm}^{-1}$ vibrational progressions suggest strongly that the ground state and excited state geometrical structures are very similar.

In the 4.2°K spectrum of the concentrated KBr pellet (Fig. 4), higher energy vibrational structure is discernible. In particular, two other $\sim 300\text{-cm}^{-1}$ progressions develop from the 16 603 and 16 664- cm^{-1} peaks (Table I). These two peaks have been assigned as $A(2) + \nu_x$ and $A(1) + \nu_x + \nu_4$, respectively, with ν_x being approximately 770 cm^{-1} . There are three reason-

able possibilities for ν_x : ν_{14} , e_{1g} CH bending (\perp); ν_2 , a_{1g} symmetrical CH bending (\perp); and ν_{27} , e_{2g} ring distortion (\parallel). Easily the most probable candidate is the e_{2g} ring distortion, because this vibrational mode should have by far the greatest overlap with the ${}^2E_{1u} \leftarrow {}^2E_{2g}$ electronic transition. Any discussion of the additional peaks and weak peaks left unassigned in Table I will be deferred until the spectral data for the other two ferricenium salts are presented.



Band system I was measured for various crystals immersed in liquid helium, and a typical 4.2°K absorption spectrum is reproduced in Fig. 5. Peak positions for the 4.2°K spectrum are given in Table III. The two lowest-energy strong peaks are separated by 180 cm^{-1} and correspond to the two leading peaks in the 77°K

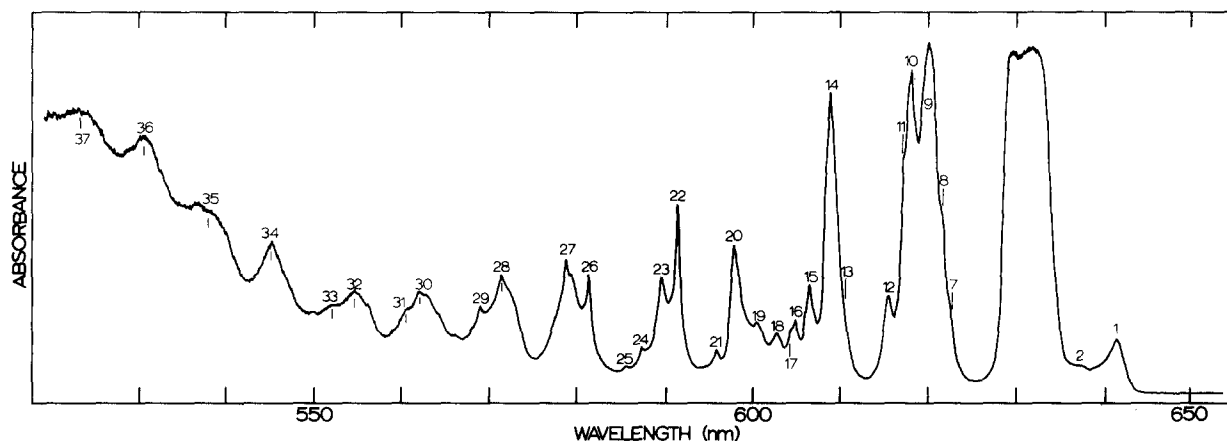


FIG. 4. Band system *I* for a high concentration KBr pellet of $[\text{Fe}(\text{C}_5\text{H}_5)_2]\text{PF}_6$ at 4.2°K (Jarrell-Ash data)—higher energy structure is discernible.

spectrum⁷ shifted by $70\text{--}90\text{ cm}^{-1}$ to lower energy. This 180 cm^{-1} spacing is the separation between the two $^2E_{1u}$ Kramers doublets.

Careful inspection of the structure in Fig. 5 shows that there are more than three $\sim 300\text{ cm}^{-1}$ vibrational progressions (Table III). Two of the progressions develop from the two electronic origins *A*(1) and *A*(2). The *A*(1) 300 cm^{-1} progression starts with (0, 0) at $15\,552\text{ cm}^{-1}$ as the most intense component and then tails off rapidly. The *A*(2) progression with its origin at $15\,731\text{ cm}^{-1}$ has as its most intense component the (1, 0) peak, and in total, this second 300 cm^{-1} progression has greater intensity than the *A*(1) 300 cm^{-1} progression. In both cases, the vibrational structure

indicates that the transitions are to an excited state with approximately the same geometry as the ground state. The average of the initial spacings in these progressions is $306 \pm 10\text{ cm}^{-1}$, a value confirming the assignment as the totally symmetric a_{1g} ring-metal-ring stretch (ν_4).

The third readily identifiable $\sim 300\text{ cm}^{-1}$ progression in the 4.2°K $[\text{Fe}(\text{C}_5\text{H}_5)_2](\text{CCl}_2\text{CO}_2\text{H})_2(\text{CCl}_3\text{CO}_2)$ spectrum starts with the strong peak at $16\,218\text{ cm}^{-1}$. In Table III, this peak has been assigned as *A*(2) + ν_{28} , that is, the (1, 0) component of a progression of the e_{2g} ring distortion (\perp) ν_{28} on the *A*(2) origin. The second component (2, 0) is seen at $16\,708\text{ cm}^{-1}$. In addition, assignment of the $16\,139\text{ cm}^{-1}$ peak as *A*(2) + ν_{16} results

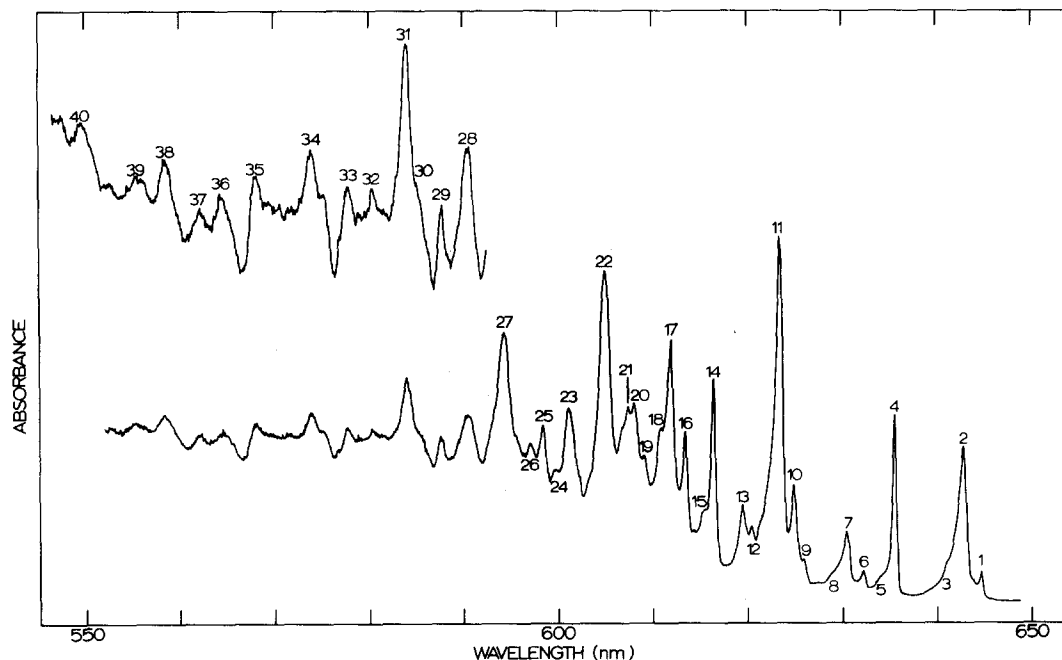


FIG. 5. Band system *I* for a single crystal of $[\text{Fe}(\text{C}_5\text{H}_5)_2]-(\text{CCl}_3\text{CO}_2\text{H})_2(\text{CCl}_3\text{CO}_2)$ at 4.2°K .

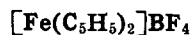
in a value of 408 cm^{-1} for the e_{1g} symmetric ring tilt (ν_{16}). A low-intensity 300-cm^{-1} progression also develops from the $16\ 139\text{-cm}^{-1}$ peak.

All but the weak peaks and shoulders have been assigned in Table III for the 4.2°K absorption spectrum of a single crystal of $[\text{Fe}(\text{C}_5\text{H}_5)_2]-(\text{CCl}_3\text{CO}_2\text{H})_2-(\text{CCl}_3\text{CO}_2)$. Perhaps the most interesting of the unassigned weak peaks are those that lie in the low-energy region. Their proximity to the $A(1)$ and $A(2)$ origins precludes an assignment as vibrational structure. We will return to these weak low-energy peaks later in the discussion.

TABLE II. Frequencies (in cm^{-1}) for the gerade vibrational modes of ferrocene.

Mode	Ref. 12	Ref. 13	Ref. 14	Description
A_{1g}				
ν_1	3099	3112	3110	sym CH stretch
ν_2	(804) ^a	815	812	sym CH bend (\perp)
ν_3	1105	1106	1105	sym ring breath
ν_4	303	311	301	sym ring- m str
A_{2g}				
ν_7	(1200)			CH deform (\parallel)
E_{1g}				
ν_{12}	3085	3089	3085	CH stretch
ν_{13}	1010	1001	999	CH bend (\parallel)
ν_{14}	(800)	815	835	CH bend (\perp)
ν_{15}	1408	1414	1412	sym C-C stretch
ν_{16}	388	393	390	sym ring tilt
E_{2g}				
ν_{23}	3085	3103	3070	C-H stretch
ν_{24}	1178	1197	1175	CH bend (\parallel)
ν_{25}	1050	1062	1059	CH bend (\parallel)
ν_{26}	1560	1358	1356	CC stretch
ν_{27}	(900)	...	892	ring dist (\parallel)
ν_{28}	(500)	600	600	ring dist (\parallel)

^a Frequencies given in parentheses were predicted from a normal coordinate analysis, but experimental values were not obtained by the authors of Ref. 12.



Liquid helium absorption spectra of band system I were recorded for samples of ferricenium tetrafluoroborate pelleted in KBr. In lowering the temperature of the pellet from 77 to 4.2°K , no change in resolution was detected (the 77°K spectrum was reported earlier⁷). Decomposition of the BF_4^- salt was noted in the KBr pellets, due perhaps to moisture. An alternative substrate was sought and finally it was found that a Nujol mineral oil mull of the BF_4^- salt gave improved resolution. A 4.2°K Nujol mull spectrum of this compound is reproduced in Fig. 6. It is clear that the resolution is not as good as we obtained for the other two salts, nevertheless, many peaks can be located in the spectrum and

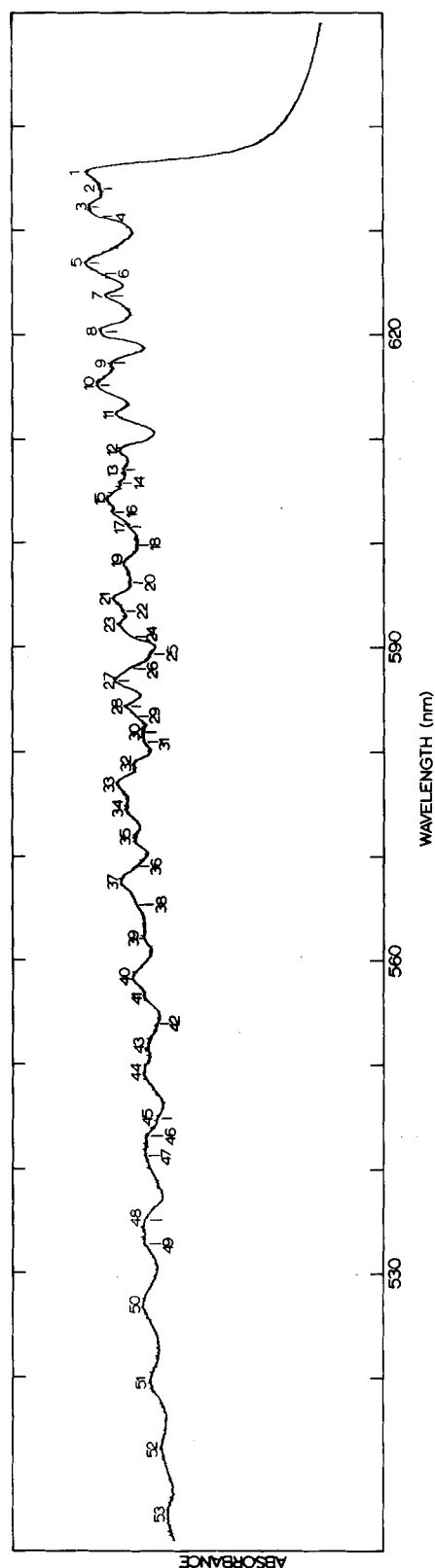


Fig. 6. Band system I for a Nujol mull of $[\text{Fe}(\text{C}_5\text{H}_5)_2]\text{BF}_4$ at 4.2°K .

TABLE III. Vibrational structure of band system *I* observed for $[\text{Fe}(\text{C}_5\text{H}_5)_2]/(\text{CCl}_3\text{CO}_2\text{H})_2/(\text{CCl}_3\text{CO}_2)$ as a single crystal at 4.2°K.

Band label	λ (Å)	$\bar{\nu}$ (cm ⁻¹) ±5 cm ⁻¹	$\Delta\bar{\nu}(a)$ ±10 cm ⁻¹	$\Delta\bar{\nu}(b)$ ±10 cm ⁻¹	$\Delta\bar{\nu}(c)$ ±10 cm ⁻¹	$\Delta\bar{\nu}(d)$ ±10 cm ⁻¹	$\Delta\bar{\nu}(e)$ ±10 cm ⁻¹	$\Delta\bar{\nu}(f)$ ±10 cm ⁻¹	Assignments
1	6448	15 509							
2	6430	15 552	origin				origin		<i>A</i> (1)
3	6413(sh)	15 593							
4	6357	15 731		origin				origin	<i>A</i> (2)
5	6342(sh)	15 768							
6	6324	15 813							
7	6306	15 858	306						<i>A</i> (1) + ν_4
8	6292(sh)	15 893							
9	6260(sh)	15 974							
10	6251	15 997					445		<i>A</i> (1) + ν_{28}
11	6236	16 036		305					<i>A</i> (2) + ν_4
12	6206	16 113							
13	6196	16 139			origin				<i>A</i> (2) + ν_{16}
14	6166	16 218				origin		487	<i>A</i> (2) + ν_{28}
15	6155	16 247							
16	6135	16 300							<i>A</i> (1) + ν_{28} + ν_4
17	6120	16 340		304					<i>A</i> (2) + $2\nu_4$
18	6110(sh)	16 367							
19	6092(sh)	16 415							
20	6082	16 442			303				<i>A</i> (2) + ν_{16} + ν_4
21	6075	16 461					464		<i>A</i> (1) + $2\nu_{28}$
22	6051	16 526				308			<i>A</i> (2) + ν_{28} + ν_4
23	6012	16 633		293					<i>A</i> (2) + $3\nu_4$
24	5998	16 672							
25	5985	16 708						490	<i>A</i> (2) + $2\nu_{28}$
26	5972	16 745			303				<i>A</i> (2) + ν_{16} + $2\nu_4$
27	5942	16 829				303			<i>A</i> (2) + ν_{28} + $2\nu_4$
28	5905	16 935		302					<i>A</i> (2) + $4\nu_4$
29	5886	16 989							<i>A</i> (2) + $2\nu_{28}$ + ν_4 (?)
30	5854(sh)	17 082							
31	5840	17 123				294			<i>A</i> (2) + ν_{28} + $3\nu_4$
32	5805	17 227		292					<i>A</i> (2) + $5\nu_4$
33	5778	17 307							
34	5739	17 425				302			<i>A</i> (2) + ν_{28} + $4\nu_4$
35	5681	17 603							
36	5644	17 718				293			<i>A</i> (2) + ν_{28} + $5\nu_4$
37	5621	17 790							
38	5584	17 908							
39	5556	17 999				281			<i>A</i> (2) + ν_{28} + $6\nu_4$
40	5496	18 195							

their relative intensities qualitatively judged. The peculiar appearance of this spectrum is due to the excessive dispersion that is encountered with a Nujol null substrate.

Peak positions and assignments for the 4.2°K ferricenium tetrafluoroborate spectrum are given in Table IV. As before, several $\sim 300\text{-cm}^{-1}$ vibrational progressions are discernible. Vibrational frequencies identifiable in this spectrum are listed in Table V along with vibrational data for the other two ferricenium salts and ferrocene. It is clear that there is fairly good agreement in the values of $\bar{\nu}_4$, $\bar{\nu}_{16}$, and $\bar{\nu}_{28}$ obtained for the ${}^2E_{1u}$ excited state of the three ferricenium compounds.

Perhaps the most important feature in the

$[\text{Fe}(\text{C}_5\text{H}_5)_2]\text{BF}_4$ spectrum is the appearance of three strong "origin" peaks *A* (1), *A* (2), and *A* (3). The separation between *A* (1) and *A* (3) is 229 cm^{-1} , and it does not appear that this can be assigned to any vibrational frequency of the ${}^2E_{1u}$ state. Similar comments pertain to the other two separations A (2)–*A* (1) = 96 cm^{-1} and A (3)–*A* (2) = 133 cm^{-1} . It is likely that the apparently unique structure in the spectrum of the BF_4^- salt is actually present in the two other compounds. That is to say, the unassigned clusters of peaks in the $[\text{Fe}(\text{C}_5\text{H}_5)_2]\text{PF}_6$ spectrum, the weak low-energy peaks observed in the $\text{CCl}_3\text{CO}_2^-$ salt, and the three strong origins and weak low-energy peak (6338 Å) of $[\text{Fe}(\text{C}_5\text{H}_5)_2]\text{BF}_4$ may be explained by a splitting of all

TABLE IV. Vibrational structure of band system *I* observed for $[\text{Fe}(\text{C}_5\text{H}_5)_2]\text{BF}_4$ in a mineral oil mull at 4.2°K.

Band label	ν (Å)	$\bar{\nu}$ (cm^{-1}) $\pm 5 \text{ cm}^{-1}$	$\Delta\bar{\nu}(a)$ $\pm 10 \text{ cm}^{-1}$	$\Delta\bar{\nu}(b)$ $\pm 10 \text{ cm}^{-1}$	$\Delta\bar{\nu}(c)$ $\pm 10 \text{ cm}^{-1}$	$\Delta\bar{\nu}(d)$ $\pm 10 \text{ cm}^{-1}$	$\Delta\bar{\nu}(e)$ $\pm 10 \text{ cm}^{-1}$	Assignments
1	6360	15 723	origin			origin	origin	<i>A</i> (1)
2	(6338) ^a	15 778						
3	6322	15 819		origin				<i>A</i> (2)
4	(6313)	15 840						
5	6269	15 952			origin			<i>A</i> (3)
6	(6259)	15 977						
7	6238	16 031	308					<i>A</i> (1) + ν_4
8	6203 ^b	16 121		302		398		$\left\{ \begin{array}{l} A(2) + \nu_4 \\ A(2) + \nu_{16} \end{array} \right\}$
9	6175(sh)	16 194					471	<i>A</i> (1) + ν_{28}
10	6152	16 255			303			<i>A</i> (3) + ν_4
11	6124	16 329	298					<i>A</i> (1) + $2\nu_4$
12	6090	16 420		299				<i>A</i> (2) + $2\nu_4$
13	(6070)	16 473						
14	6058(sh)	16 506				385		<i>A</i> (2) + $2\nu_{16}$
15	6042	16 551			296			<i>A</i> (3) + $2\nu_4$
16	6027	16 592						
17	6015	16 625	296					<i>A</i> (1) + $3\nu_4$
18	(5998)	16 672						
19	5981	16 720		300				<i>A</i> (2) + $3\nu_4$
20	(5962)	16 773						
21	5947	16 815						
22	(5934)	16 852			301			<i>A</i> (3) + $3\nu_4$
23	5921	16 889						
24	5908(sh)	16 926						
25	5893	16 969						
26	5880(sh)	17 007		287				<i>A</i> (2) + $4\nu_4$
27	5868	17 040						
28	5844	17 112						
29	5833(sh)	17 144						
30	5819	17 185						
31	5808	17 208						
32	5791(sh)	17 268						
33	5771	17 328						
34	5744	17 409						
35	5716	17 495						
36	5693(sh)	17 566						
37	5675	17 621						
38	5655	17 684						
39	5621	17 790						
40	5584	17 908						
41	5562	17 974						
42	5540	18 050						
43	5520	18 118						
44	5491	18 212						
45	5450	18 347						
46	5433	18 406						
47	5416	18 466						
48	5352	18 686						
49	5330	18 764						
50	5261	19 008						
51	5198	19 240						
52	5131	19 489						
53	5066	19 739						

^a A peak that is not well resolved, but is strongly suggested by the band contour, is enclosed in parentheses.^b This peak appears to be comprised of two similarly intense, incompletely resolved components.

TABLE V. Comparison of band system *I* vibrational spacings with Raman data for ferrocene.

	$\bar{\nu}_4$ (cm ⁻¹)	$\bar{\nu}_{16}$ (cm ⁻¹)	$\bar{\nu}_{28}$ (cm ⁻¹)
Ferrocene			
Raman (averaged) ^a	305	390	600
Compound			
[Fe(C ₅ H ₅) ₂]PF ₆	303 ^b	not obs	not obs
[Fe(C ₅ H ₅) ₂] (CCl ₃ CO ₂ H) ₂	307	408	445 from <i>A</i> (1) 487 from <i>A</i> (2)
(CCl ₃ CO ₂) ₂			
[Fe(C ₅ H ₅) ₂]BF ₄	304	398	471

^a See Table II.^b All frequencies were calculated from the initial spacings of each assigned vibrational progression.

A(1) and *A*(2) progressions by exchange interactions between neighboring ferricenium ions.

If there is exchange interaction between ferricenium ions, the compound whose crystalline unit cell contains the greatest number of molecules not related by translational symmetry should show the greatest peak splitting.¹⁵ No crystal data for [Fe(C₅H₅)₂]BF₄ have been obtained, but x-ray results on both the PF₆⁻ and CCl₃CO₂⁻ salts are available. A complete x-ray crystal structure analysis established that the trichloroacetate salt is in the *P*2₁/*m* space group with two molecules per unit cell, whereas crystals of [Fe(C₅H₅)₂]PF₆ are *P*2₁/*c* with four molecules per unit cell.¹⁶ Thus, for splitting due to exchange interactions, a more complicated spectrum is likely in the PF₆⁻ case. The fact that there are more unassigned features in the important low energy region of the spectrum of the PF₆⁻ salt is qualitatively consistent with the crystal structural information.

²*E*_{1u} Ferricenium Bonding

We have already noted that the ²*E*_{1u} ferricenium geometrical structure probably does not differ significantly from that in the ground state (²*E*_{2g}). As x-ray structure determinations have shown that the iron–ring distance is about the same in ¹*A*_{1g} ferrocene^{17,18} and ²*E*_{2g} ferricenium,^{16,19,20} this distance must also be approximately correct for ²*E*_{1u} ferricenium. Further, the fact that the totally symmetric ring–metal–ring stretch (ν_4) has essentially the same value for ²*E*_{1u} ferricenium and ¹*A*_{1g} ferrocene, as set out in Table V, attests to the close similarity in ring–metal bond strength in the two cases. We may conclude therefore that the iron *e*_{1u}(4*p*_x, 4*p*_y) orbitals do not participate significantly in the ring–metal bonding, as the only electronic configurational difference in ¹*A*_{1g} ferrocene and ²*E*_{1u} ferricenium is the occupancy of the lower-energy *e*_{1u} molecular orbital level.

Data in Table V taken from the 4.2°K spectra of the CCl₃CO₂⁻ and BF₄⁻ salts establish that the *e*_{1g} symmetric ring tilt (ν_{16}) for ²*E*_{1u} ferricenium has a value of ~403 cm⁻¹, as compared to 390 cm⁻¹ for ¹*A*_{1g} ferrocene.

This result provides additional support for the conclusion that the occupied *e*_{1u} level is almost entirely localized on the cyclopentadienyl rings. The *e*_{1u} level is further characterized by the identification of the *e*_{2g} ring distortion (\perp) ν_{28} in the vibrational structure observed for the trichloroacetate and tetrafluoroborate compounds. A value of 450–490 cm⁻¹ has been found for ν_{28} (²*E*_{1u}), which is much lower than the corresponding frequency (~600 cm⁻¹) for ¹*A*_{1g} ferrocene (Table V). The reduction in the perpendicular ring deformation frequency in ²*E*_{1u} ferricenium is consistent with substantial intraring bonding character of the *e*_{1u} level.

It is interesting to examine a representative selection^{21–27} of the many molecular orbital treatments of ferrocene and ferricenium in the light of our vibrational analysis of ²*E*_{1u} ferricenium. In 1954 Moffitt suggested²³ that the iron–ring bonding could be attributed mainly to overlap of *e*_{1g} metal (3*d*_{xy}, 3*d*_{yz}) and cyclopentadienyl orbitals, and he proposed further that any contribution involving mixing of 4*p*_x and 4*p*_y orbitals with *e*_{1u} cyclopentadienyl orbitals was likely to be very small. Dunitz and Orgel expressed some reservations about neglecting 4*p*_x and 4*p*_y orbitals in their semiquantitative bonding scheme, but they came to the same conclusion as Moffitt²³ concerning the importance of the *e*_{1g} orbitals. Both Jaffe²¹ and Ruch²⁴ incorporated some mixing of the iron 4*p*_x and 4*p*_y with ring orbitals, but the qualitative nature of their molecular orbital models of ferrocene does not allow any prediction of the relative importance of this interaction.

Full details of three self-consistent-field (SCF MO) calculations of ferrocene have been reported. Dahl and Ballhausen²⁶ used a nonempirical form of the zero-differential-overlap method and found fairly extensive mixing of the iron 4*p*_x and 4*p*_y orbitals with the ring *e*_{1u} orbitals. The semiempirical SCF MO calculations of Shustorovich and Dyatkina²⁵ also predicted substantial mixing. In a very recent *ab initio* SCF MO treatment, Coutière *et al.*²⁷ calculated that 0.24 electrons are transferred from the ring to the metal *e*_{1u} orbitals in the ground state of ferrocene. Thus it would appear that the available SCF MO calculations have overemphasized the effectiveness of the 4*p*_x and 4*p*_y orbitals of iron in bonding to the cyclopentadienyl rings.

In summary, our conclusion, based on experiment, that the lower *e*_{1u} level is ring localized, and not involved in bonding to the metal 4*p*_x and 4*p*_y orbitals, accords well with some of the earliest ideas about the electronic structure of ferrocene, in particular those of Moffitt²³ and Dunitz and Orgel.²² It is probable, therefore, that the iron and cyclopentadienyl orbitals of *e*_{1g} symmetry play by far the most important role in ring–metal binding.

ACKNOWLEDGMENTS

Research at the California Institute of Technology was supported by the National Science Foundation. We thank Professor C. J. Ballhausen, H. Johansen, and Dr. Albert Mortola for helpful comments.

- *School of Chemical Sciences, University of Illinois, Urbana, Ill. 61801.
- [†]Arthur Amos Noyes Laboratory of Chemical Physics, California Institute of Technology, Pasadena, Calif. 91109.
- [‡]NSF Summer Trainee, 1972; ESSO Fellow in Chemistry, 1971–1972.
- [§]Contribution No. 4530.
- ¹D. N. Hendrickson, Y. S. Sohn, and H. B. Gray, *Inorg. Chem.* **10**, 1376 (1971).
- ²R. Prins and F. J. Reinders, *J. Am. Chem. Soc.* **91**, 4929 (1969).
- ³A. Horsfield and A. Wassermann, *J. Chem. Soc. (Lond.)* **1970**, 3202.
- ⁴R. Prins and A. R. Korswagen, *J. Organomet. Chem.* **25**, C75 (1970).
- ⁵Y. S. Sohn, D. N. Hendrickson, and H. B. Gray, *J. Am. Chem. Soc.* **92**, 3233 (1970).
- ⁶R. Prins, *Chem. Commun.* **1970**, 280.
- ⁷Y. S. Sohn, D. N. Hendrickson, and H. B. Gray, *J. Am. Chem. Soc.* **93**, 3603 (1971).
- ⁸D. A. Levy and L. E. Orgel, *Mol. Phys.* **4**, 93 (1961).
- ⁹D. R. Scott and R. S. Becker, *J. Phys. Chem.* **69**, 3207 (1965).
- ¹⁰M. Aly, R. Bramly, J. Upadhyay, A. Wassermann, and P. Woolliams, *Chem. Commun.* **1965**, 404; M. Aly, D. V. Banthorpe, R. Branley, R. E. Cooper, D. W. Jopling, J. Upadhyay, A. Wassermann, and P. R. Woolliams, *Monatsh. Chem.* **98**, 887 (1967); B. V. Banthorpe, B. V. Charlwood, and A. Wassermann, *Chem. Commun.* **1972**, 294.
- ¹¹R. Prins and A. G. T. G. Kortbeek, *J. Organomet. Chem.* **33**, C33 (1971).
- ¹²E. R. Lippincott and R. D. Nelson, *Spectrochim. Acta* **10**, 307 (1958).
- ¹³D. Hartley and M. J. Ware, *J. Chem. Soc. A* **1969**, 138.
- ¹⁴T. V. Long and F. R. Huege, *Chem. Commun.* **1968**, 1239.
- ¹⁵D. S. McClure, *Electronic Spectra of Molecules and Ions in Crystals* (Academic, New York, 1959).
- ¹⁶A. W. Schlueter and H. B. Gray (unpublished results).
- ¹⁷E. A. Seibold and L. E. Sutton, *J. Chem. Phys.* **23**, 1967 (1955).
- ¹⁸J. D. Dunitz, L. E. Orgel, and A. Rich, *Acta Crystallogr.* **9**, 373 (1956).
- ¹⁹T. Berstein and F. H. Herbststein, *Acta Crystallogr. B* **24**, 1640 (1968).
- ²⁰R. C. Petterson, Ph.D. thesis, University of California, Berkeley, Calif., 1966.
- ²¹H. H. Jaffe, *J. Chem. Phys.* **21**, 156 (1953).
- ²²J. D. Dunitz and L. E. Orgel, *Nature (Lond.)* **171**, 121 (1953); *J. Chem. Phys.* **23**, 954 (1955).
- ²³W. Moffitt, *J. Am. Chem. Soc.* **76**, 3386 (1954).
- ²⁴E. Ruch, *Recl. Trav. Chim. Pays-Bas* **75**, 638 (1956).
- ²⁵E. M. Shustorovich and M. E. Dyatkina, *Dokl. Akad. Nauk SSSR* **128**, 1234 (1959); *Dokl. Akad. Nauk SSSR* **131**, 113 (1960); *Dokl. Akad. Nauk SSSR* **133**, 141 (1960).
- ²⁶J. P. Dahl and C. J. Ballhausen, *K. Dan. Vidensk. Selsk. Mat.-Fys. Medd.* **1961**, 33.
- ²⁷M.-M. Coutière, J. Demuynck, and A. Veillard, *Theor. Chim. Acta* **27**, 281 (1972).